

**FREQUENCY COMPARISON (H_MASER 40 0805) - (BNM-SYRTE-FO2)
From MJD 53489 to MJD 53504**

The primary frequency standard BNM-SYRTE-FO2 was compared to the hydrogen Maser (40 0805) of the laboratory, from MJD 53489 to MJD 53504.

The mean frequency differences measured between the hydrogen Maser 40 0805 and fountain FO2 during this period is given in table 1. Additionally, the mean frequency between hydrogen Masers 40 0816 and 40 0805 are evaluated during the same period of measurement.

Period (MJD)	$y(\text{HMaser}_{40\ 0805} - \text{FO2})$ (7)	u_B (2)	u_A (7)	$u_{\text{link} / \text{maser}}$ (4)
53489 – 53504	+ 5736,61	7,32	0,47	1,10
53489 - 53504	$y(\text{HMaser}_{40\ 0805} - \text{HMaser}_{40\ 0816})$ +2455,93 (8)	0,05	0,03	

Table 1: Results of the comparison in 1×10^{-16} unit.

Figure 1 collects the measurements of fractional frequency differences during the 28th April to 14th May 2005 period. Error bars represent the combined statistical and systematic uncertainties. The measurements are corrected for the systematic frequency shifts listed below.

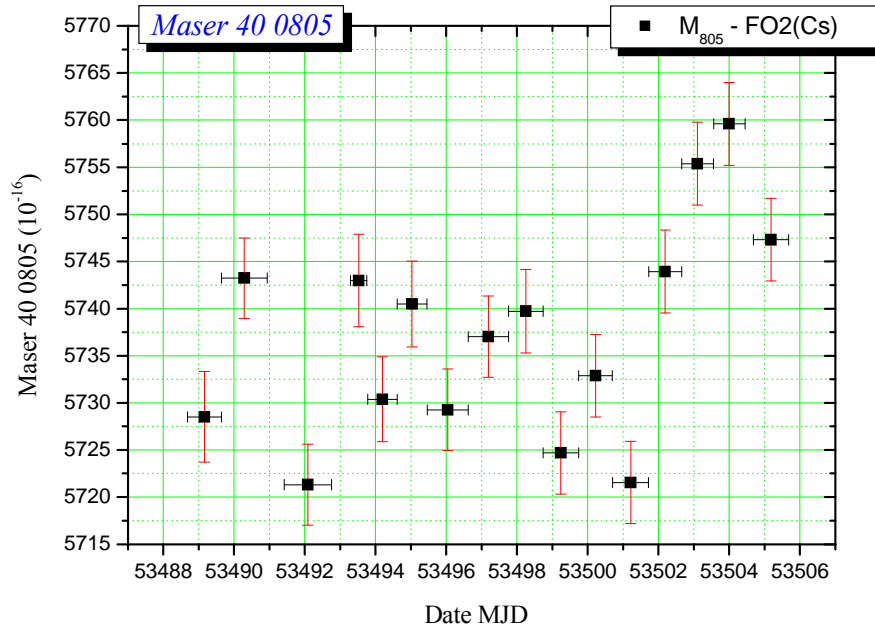


Figure 1: fractional frequency differences between H_Maser40 0805 & FO2 from MJD 53489 to MJD 53504

Table of measurements is given bellow (table 2) and a synthesis of calculation on table 3.

Start UTC dates unit MJD	Start Local dates unit H:M	Duration H:M	Mean fractional frequency differences $y_{Maser} - y_{FO2}$	type A uncertainties	
				σ_{Stat}	$\sigma_{Collision}$
53488,68807	28/04/2005 18:30	22:55	5,73085E-13	1,78E-16	2,12E-16
53489,64921	29/04/2005 17:34	30:59	5,74556E-13	1,07E-16	1,29E-16
53491,42046	01/05/2005 12:05	32:07	5,72366E-13	1,08E-16	1,32E-16
53493,29558	03/05/2005 09:05	11:08	5,74532E-13	1,88E-16	2,24E-16
53493,78264	03/05/2005 20:47	19:59	5,73272E-13	1,4E-16	1,69E-16
53494,61551	04/05/2005 16:46	20:13	5,74284E-13	1,43E-16	1,79E-16
53495,46235	05/05/2005 13:05	27:51	5,7316E-13	1,16E-16	1,4E-16
53496,62280	06/05/2005 16:56	27:25	5,73935E-13	1,13E-16	1,41E-16
53497,76913	07/05/2005 20:27	23:17	5,74205E-13	1,28E-16	1,57E-16
53498,74444	08/05/2005 19:52	23:55	5,72703E-13	1,21E-16	1,49E-16
53499,74159	09/05/2005 19:47	23:01	5,73522E-13	1,24E-16	1,54E-16
53500,70716	10/05/2005 18:58	24:13	5,72389E-13	1,2E-16	1,49E-16
53501,72146	11/05/2005 19:18	22:21	5,74627E-13	1,25E-16	1,53E-16
53502,65242	12/05/2005 17:39	21:37	5,7577E-13	1,25E-16	1,54E-16
53503,56069	13/05/2005 15:27	21:18	5,76194E-13	1,25E-16	1,55E-16
53504,68248	14/05/2005 18:22	24:01	5,74965E-13	1,22E-16	1,5E-16

Table 2: Measurements H_Maser40 0805 - FO2 from MJD 53379 to 53399

Dates Duration & Measurement Rate	Mean frequency difference normalized $y_{Maser} - y_{FO2}$ (1)	type A uncertainty $\sigma_{Stat} \& \sigma_{Collision}$	Uncertainty due to the dead times $\sigma_{deadTime}$ (4)
Start date MJD UTC 53488,68807 Stop date MJD UTC 53505,68264 Total duration : 16,99457 d Total measurements 15,670833 d Measurement Rate: 92,21%	Standard Mean $\bar{y} = 5737,39 \times 10^{-16}$ Weighted Mean (5): $\bar{y} = 5737,08 \times 10^{-16}$ Linear fit regression (6): $\bar{y} = 5736,47 \times 10^{-16}$ High order polynomial fit (6): $\bar{y} = 5737,03 \times 10^{-16}$ Mean from Phase differences (7): $\bar{y} = 5736,61 \times 10^{-16}$	By Weighted Mean (5) $\sigma_A = 0,49 \times 10^{-16}$ By Linear fit regression(6) $\sigma_y = 0,55 \times 10^{-16}$ By High order Polynomial fit (6) $\sigma_y = 0,55 \times 10^{-16}$ From Phase differences (7) $\sigma_A = 0,47 \times 10^{-16}$	$\sigma_{deadTime} =$ 0,45 10^{-16}

Table 3: Statistics of measurements

- (1) Fractional frequency difference obtained after systematic relative frequency shifts correction:

$$y_{Maser - FOM} = \frac{\delta(\nu)_{Zeeman2}}{\nu_0} + \frac{\delta(\nu)_{BlackBody}}{\nu_0} + \frac{\delta(\nu)_{Collision + CavityPulling}}{\nu_0} + \frac{\delta(\nu)_{redshift}}{\nu_0} - \frac{f_{mesure}}{\nu_0}$$

with $\nu_0 := 0.9192631770 \cdot 10^{10}$. The fractional mean frequency is calculated by four ways as mentioned in table 3 in order to have comparison between statistical computation such as standard mean, weighted mean, with a linear fit and with phase differences.

- (2) Systematic uncertainty $\sigma_B = u_B$ in which statistical effect of cold collisions and cavity pulling is removed (see **Annex 1**)

$$\sigma_B = \left(\sigma_{Zeeman2}^2 + \sigma_{BlackBody}^2 + \sigma_{Collision_{Syst}}^2 + \sigma_{Microwave_{Spectrum}}^2 + \sigma_{Microwave_{Leakage}}^2 + \sigma_{Ramsey_{Rabi}}^2 + \sigma_{Recoil}^2 + \sigma_{second_{Doppler}}^2 + \sigma_{Background_{collisions}}^2 + \sigma_{Redshift}^2 \right)^{(1/2)}$$

- (3) Statistical uncertainty $\sigma_A = u_A$, in which is taken into account the statistical uncertainty on each measurement σ_{Stat_i} and statistical effect on the cold collisions and Cavity Pulling measurement $\sigma_{Collision_i}$ (see **Annex 4** Linear Regression on the

frequency measurements & **Annex 5**):
$$\sigma_A = \sqrt{\frac{1}{\sum_{i=1}^n \frac{1}{\sigma_{Stat_i}^2 + \sigma_{Collision_i}^2}}}$$

- (4) Uncertainty due to the link between H_Maser and the fountain FO2 $u_{link_Maser} = \sqrt{\sigma_{link_Lab}^2 + \sigma_{dead_time}^2}$ where $\sigma_{link_Lab} = 0.1 \cdot 10^{-15}$ and σ_{dead_time} is the uncertainty due to the dead times during measurements (see **Annex 3**)

- (5) Weighted Mean by statistical uncertainty on each measurement

$$y_j := \frac{\sum_{i=1}^{n_j} \frac{y_i}{\sigma_{Ai}^2}}{\sum_{i=1}^{n_j} \frac{1}{\sigma_{Ai}^2}}$$

where $\sigma_A = \sqrt{\frac{1}{\sum_{i=1}^n \frac{1}{\sigma_{Ai}^2}}}$ with $\sigma_{Ai} = \sqrt{\sigma_{Stat_i}^2 + \sigma_{Collision_i}^2}$

- (6) Mean frequency obtained by a linear fit by weighted least squares with statistical uncertainty on each measurement and by an high order polynomial fit (see **Annex 4**).
- (7) Mean frequency obtained by phase differences that is the retained result (see **Annex 5**).
- (8) Mean frequency obtained by first phase differences between Masers 40 0805 and 40 0816 (see **Annex 6**).

ANNEX 1

Uncertainties of systematic effects in the FO2 fountain

Systematic effects taken into account are the quadratic Zeeman, the Black Body, the cold collision and cavity pulling corresponding to the systematic part (see Annex 2), the microwave spectral purity and the microwave leakage, the Ramsey Rabi pulling, the recoil, the 2nd Doppler and the background collisions. Each of these effects is affected by an uncertainty. The uncertainty of the red shift effect is also included in the systematic uncertainty budget and gives

$$\sigma_B = \left(\sigma_{Zeeman2}^2 + \sigma_{BlackBody}^2 + \sigma_{Collision_{Syst}}^2 + \sigma_{Microwave_Spectrum_Leakage}^2 + \sigma_{first_Doppler}^2 + \sigma_{Ramsey_Rabi}^2 + \sigma_{Recoil}^2 + \sigma_{second_Doppler}^2 + \sigma_{Background_collisions}^2 + \sigma_{Redshift}^2 \right)^{(1/2)}$$

Here are mentioned the uncertainties of the different effects (see **Annex 2** and **[ref, 1]**):

Quadratic Zeeman effect	:	$\sigma_{Zeeman2} := 0.98 \cdot 10^{-17}$	(continuously measured)
Black Body effect	:	$\sigma_{BlackBody} := 0.25 \cdot 10^{-15}$	(calculated)
Systematic Collisional effect	:	$\sigma_{Collision_{Syst}} := 0.289 \cdot 10^{-15}$	(continuously measured see annex 2)
Microwave Spectrum purity & Leakage effect	:	$\sigma_{Microwave_Spectrum_Leakage} := 0.45 \cdot 10^{-15}$	(measured)
First order Doppler effect	:	$\sigma_{first_Doppler} := 0.38 \cdot 10^{-15}$	(calculated and measured)
Rabi-Ramsey effect	:	$\sigma_{Ramsey_Rabi} < 0.10 \cdot 10^{-15}$	(calculated)
Recoil effect (see [ref, 3])	:	$\sigma_{Recoil} := 0.10 \cdot 10^{-15}$	(calculated)
Second order Doppler effect	:	$\sigma_{second_Doppler} := 0.8 \cdot 10^{-17}$	(calculated)
Background effect	:	$\sigma_{Background_collisions} := 0.10 \cdot 10^{-15}$	(evaluated)
Red shift effect	:	$\sigma_{Redshift} = 0.1 \cdot 10^{-15}$	(calculated)

For the whole April-May 2005 period it gives

$$\rightarrow \boxed{\sigma_B = 0.732 \cdot 10^{-15}}$$

1 - Measurement of the collisional frequency shift and the cavity pulling

Collisional shift takes into account the effect of the collisions between cold Caesium atoms and the effect of "Cavity Pulling" whose influence also depends on the number of atoms. This effect is measured in a differential way during each integration and its determination thus depends on the duration of the measurement and on the stability of the clock, thus the uncertainty on the determination of the collisional shift is mainly of statistical nature. To the statistical uncertainty, we add a type B uncertainty of 1% of frequency shift resulting from the imperfection of the adiabatic passage method (see the article [ref. 4]).

Figure 2 visualizes the relative frequency shift due to the effect of the collisions and "Cavity Pulling" of the atomic fountain FO2 taken in low density, between the MJD 53489 and 53505 with the $\sigma_{Collision(i)}$ statistical uncertainty of each measurement, given in table 2.

Figure 3 shows the Allan deviation of a differential measurement using high and half atom density fountain configurations during MJD 53489 to MJD 53505, in order to correct of the cold collisional shift for this period. FO2 was operated alternatively (every 50 clock cycles) at low atomic density (red diamond) and high density (black square) against the cryogenic oscillator weakly phase locked on the H_Maser805. The measured density ratio between low and high densities is $0,50110632 \pm 0,0000393$. The frequency difference between both densities is used to determine the collisional coefficient which is used to correct each data point. The blue triangle points represent the Allan deviation of the frequency difference between low and high densities when the points are corrected. The Allan deviation varies as $\tau^{-1/2}$ and reaches 10^{-16} after 100000s.

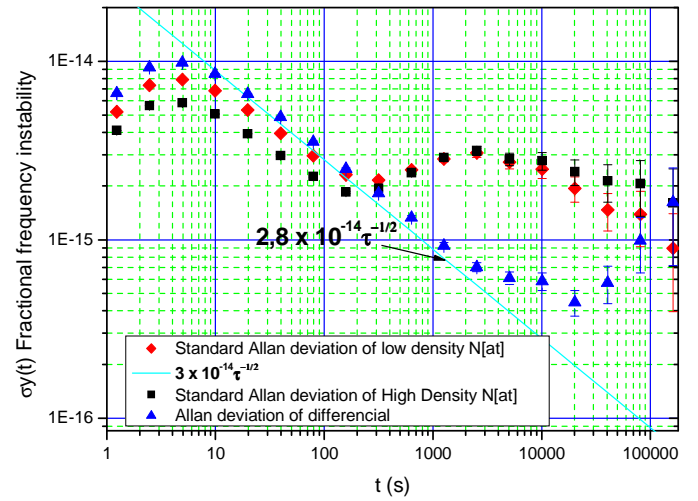
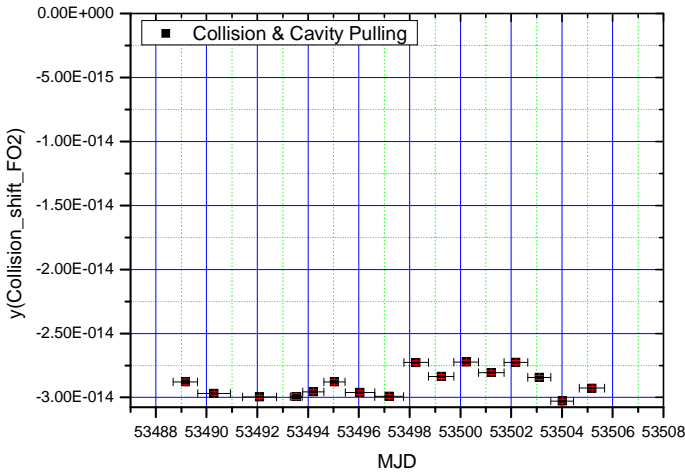


Figure 2: Fractional frequency shift due to cold collisions and Cavity Pulling from MJD 53489 to MJD 53505

Figure 3: Allan deviation of measurements of the shift frequency in high and low atom density and their differences during MJD 53489 to MJD 53505

The weighted mean $y_{Collision_{moy}} = \frac{\sum_{i=1}^n \frac{y_{Collision_i}}{\sigma_{Collision_i}^2}}{\sum_{i=1}^n \frac{1}{\sigma_{Collision_i}^2}}$ of collisional shift gives for April May is $y_{Collision_{moy}} := -0.28930 \cdot 10^{-13}$

The systematic effect of these shifts is evaluated by the 1% part of the mean frequency collisional shift during April May:

$$\sigma_{Collision_{Syst}} = \frac{1}{100} |y_{Collision_{moy}}| = \sigma_{Collision_{Syst}} := 0.28930 \cdot 10^{-15}$$

This value is taking into account in the systematic uncertainty evaluation σ_B (see Annex 1).

2 - Measurement of the 2nd order Zeeman frequency shift

Every 20 minutes the frequency of the central fringe of the field linearly dependant transition $|F=3, m_F=1\rangle \rightarrow |F=4, m_F=1\rangle$ is measured. This frequency is directly proportional to the field as $\delta(\nu_{11})=K_{Z1}B$ with $K_{Z1} = 7,0084 \text{ Hz.nT}^{-1}$ (see [ref. 5] vol. 1 p37 table 1.1.7(a)). In the fountain, the transition $|F=3, m_F=0\rangle \rightarrow |F=4, m_F=0\rangle$ is shifted by quadratic Zeeman effect and depend on squared magnetic field as $\delta(\nu_{00})=K_{Z2}B^2$ with $K_{Z2} = 42,745 \text{ mHz.}\mu\text{T}^{-2}$ (see [ref. 5] vol. 1 p37 table 1.1.7(a)). Knowing K_{Z1} and measuring $\delta(\nu_{11})$ allow good

estimation of Zeeman quadratic shift as $\delta(\nu_{00}) = K_{Z2} \left(\frac{\delta(\nu_{11})}{K_{Z1}} \right)^2$. The relative quadratic Zeeman frequency shift is calculated by

$\frac{\delta(\nu_{00})}{\nu_0} = 427,45 \times 10^{-6} \left(\frac{\delta(\nu_{11})}{700,84} \right)^2$ with $\delta(\nu_{11})$ in Hz unit and $\nu_0 = 9192631770 \text{ Hz}$. And the uncertainty is evaluated

by $\frac{\Delta(\delta(\nu_{00}))}{\nu_0} = 427,45 \times 10^{-6} \times \frac{2 \times \bar{B} \times \Delta(B)}{\nu_0}$ with B in mG. Figure 4 displays the tracking of the central fringe during MJD 53489 to

MJD 53506. This shows the good stability of the magnetic field in the interrogation zone. The frequency variation is taken as in an interval of standard deviation $\pm 0,0363 \text{ Hz}$. When taking the standard deviation of variation of the magnetic field $\Delta(B)$ over the whole measurement period as the field uncertainty, we find $5,18 \text{ pT}$. The corresponding uncertainty of the correction of the second order Zeeman effect is $0,0976 \times 10^{-16}$. During each period of about 24h of integration (see table 2) an evaluation of the Zeeman effect is calculated assorted with an uncertainty averaged from the tracking of the central fringe during this interval duration of about 24h.

For $MI := 1420.02 \text{ Hz}$, relative quadratic Zeeman shift $\delta_{\nu_{Zeeman2}} = 0.1908959 \cdot 10^{-12}$, $\sigma_{Zeeman2} := 0.976 \cdot 10^{-17}$

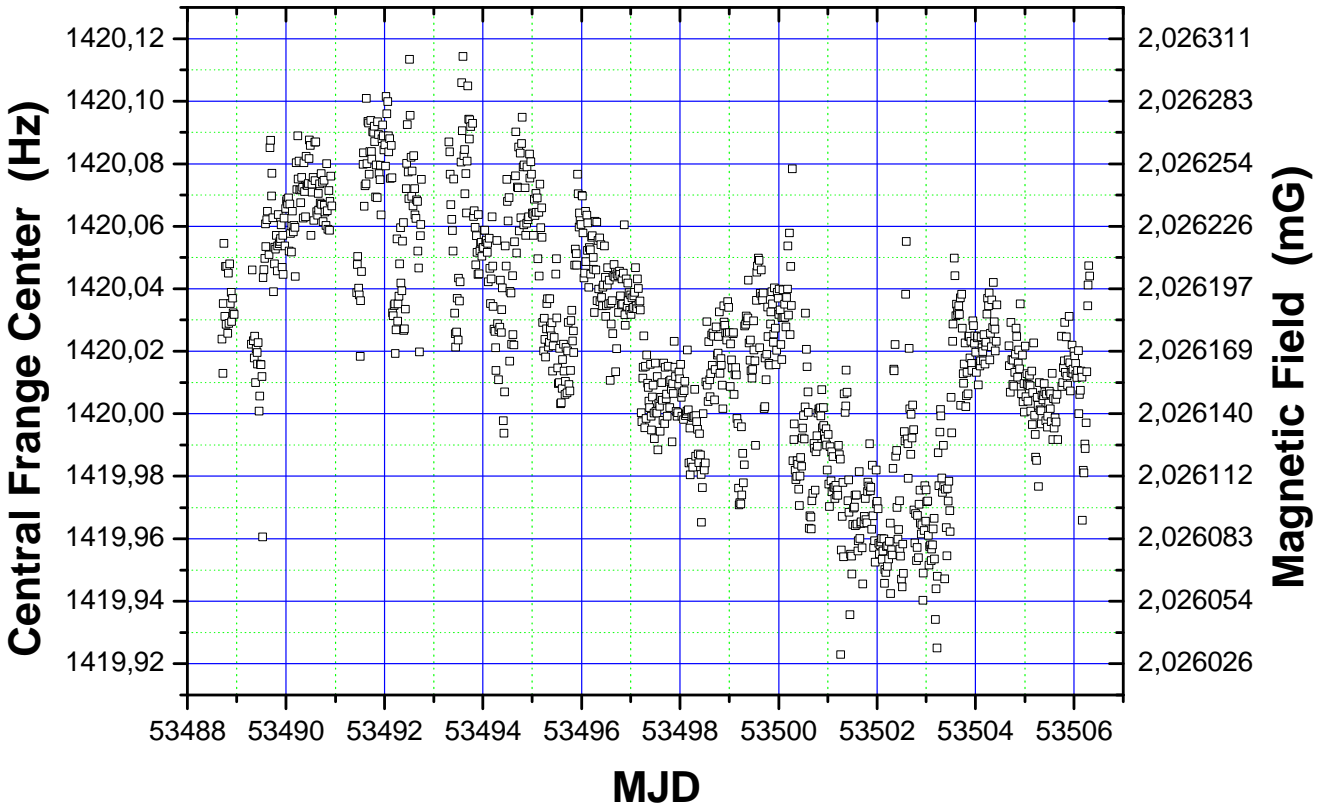


Figure 4: tracking of the central fringe from MJD 53489 to MJD 53506

3 - Measurement of the Blackbody Radiation shift

An ensemble of 3 platinum thermistors monitors the temperature and its gradient inside the vacuum chamber. The average temperature is $\sim 25,6^\circ\text{C}$ with a gradient smaller than 1 K along the atom trajectory. The correction is

$$\left(\frac{\delta(\nu)}{\nu_0}\right)_{\text{Blackbody}} = \frac{0.0001573 \left(\frac{T}{300} + 0.9105000000\right)^4 \left(1 + 0.014 \left(\frac{T}{300} + 0.9105000000\right)^2\right)}{\nu_0} = -0.17062 \cdot 10^{-13} \pm 0.25 \cdot 10^{-15}$$

4 - Effect of the Microwave Spectrum effect and leakage effect

The clock frequency is measured as a function of the microwave power. Every 50 cycles the atom interrogation is alternated between 4 configurations of $\pi/2$, low density and high density, and $3\pi/2$, low density and high density. It allows extrapolating and removing the variation of the collision shift in the comparison between $\pi/2$ and $3\pi/2$ pulses. We find

$$\frac{\delta(\nu)_{\text{Microwave_Spectrum_Leakage}}}{\nu_0} = -0.44 \cdot 10^{-15} \pm 0.45 \cdot 10^{-15}$$

5 - Measurement of the residual 1st order Doppler effect

We determined the frequency shifts caused by asymmetry of the coupling coefficients of the two microwave feedthroughs and the error on the launching direction by coupling the interrogation signal either “from the right” or “from the left” or symmetrically into the cavity. The measured shift is

$$\left(\frac{\delta(\nu)}{\nu_0}\right)_{\text{first_Doppler}} = 0.45 \cdot 10^{-14} \pm 0.38 \cdot 10^{-15}$$

In FO2 fountain we feed the cavity symmetrically at 1% level both in phase and in amplitude. This shift is thus reduced by a factor of 100 and became negligible. The quadratic dependence of the phase becomes dominant. A worse case estimate based on [ref. 6] gives fractional frequency shift of 3×10^{-16} which we take as uncertainty due to the residual 1st order Doppler effect.

6 – Rabi and Ramsey effect and Majorana transitions effect

An imbalance between the residual populations and coherences of $m_F < 0$ and $m_F > 0$ states can lead to a shift of the clock frequency estimated to few 10^{-18} for a population imbalance of 10^{-3} that we observe in FO2 (see [ref. 7] and [ref. 8]).

7 – Microwave recoil effect

The shift due to the microwave photon recoil was investigated in [ref. 3]. It is smaller than $1,4 \times 10^{-16}$.

8 – Gravitational red-shift and 2nd order Doppler shift

The relativistic effect is evaluated as: $\frac{\delta(\nu)_{\text{redshift}}}{\nu_0} = 0.625 \cdot 10^{-14}$ with an uncertainty $\sigma_{\text{Redshift}} = 0.1 \cdot 10^{-15}$

The 2nd order Doppler shift is less than $0,08 \times 10^{-16}$.

9 – Background collisions effect

The vacuum pressure inside the fountains is typically a few 10^{-8} Pa. Based on early measurements of pressure shift (see [ref. 5]) the frequency shift due to collisions with the background gas is $< 10^{-16}$.

See [ref. 9] for recent evaluations of systematic effects of FO2 fountain.

Uncertainty due to the dead time during the measurements

A statement of the distribution of the idle periods of measurements of FO2 is represented in figure 5,

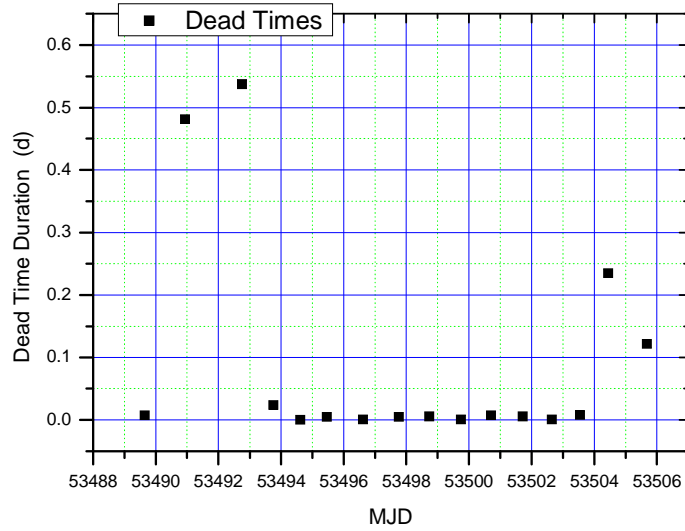


Figure 5: Dead Times on measurements of $y(H_Maser40\ 0805 - FO2)$ over the period MJD 53489 to 53505

For the period of the MJD 53405 until the MJD 53509 (4th February to 19th May 2005), the variations of phase between hydrogen Maser 40 0805 and the hydrogen Maser 40 0816 were sampled every 100s. After removing a quadratic fit on phase variations to carry out the calculation of standard deviation in the temporal field, we have evaluated the uncertainty associated with the H_Maser according to time (by step of 100s). We have obtained the phase variations between H_Maser 40 0805 and the H_Maser 40 0816 plotted in figure 6.

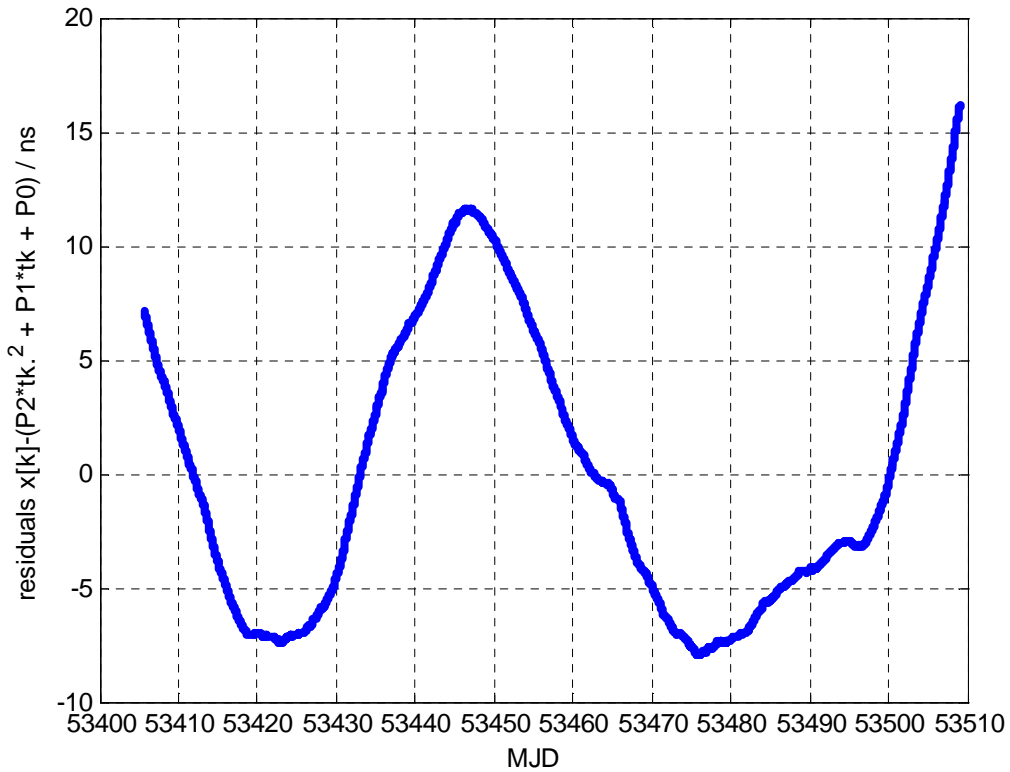


Figure 6: phase data $x(Maser805-Maser816)$ quadratic fit removed $x(H805-H816)$ MJD 53405 to MJD 53509

Frequency stability analyses were performed using the overlapping Allan deviation on frequency data and represented from 4th February to 19th May 2005 in figure 7 and similarly time stability analyses with a time deviation were computed and represented in figure 8 .

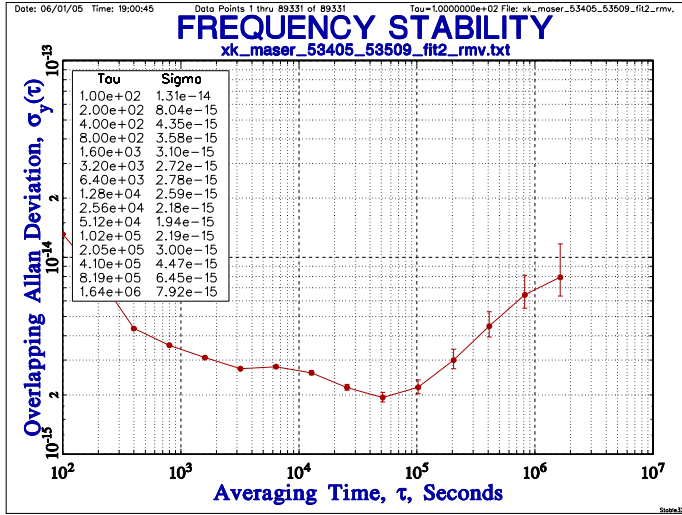


Figure 7: frequency stability analyzes $x(\text{HMaser805} - \text{HMaser816})$ from MJD 53405 to MJD 53509

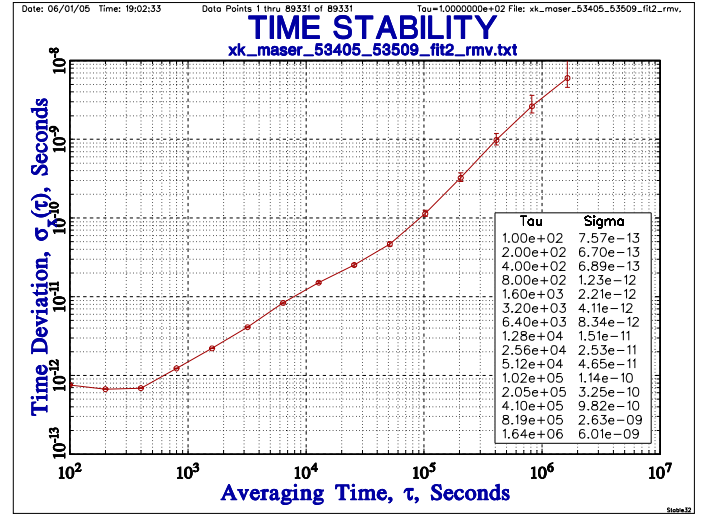


Figure 8: time stability analyzes from $x(\text{HMaser805} - \text{HMaser816})$ from MJD 53405 to MJD 53509

Table 4 provides the standard deviations of the phase fluctuations of the hydrogen Maser 40 0805 with respect to the hydrogen Maser 40 0816 associated to each dead time according to their duration. The quadratic sum gives

$$\sum_{i=1}^{16} \sigma_x(\tau_m(i))^2 = 0.4374335380 \cdot 10^{-20}$$

The April May 2005 period of FO2 measurements is 16,99457 days or $T := 0.1468330848 \cdot 10^7$ seconds. We find the standard deviation of the fluctuations of frequency due to the dead times in measurements by the ratio

$$\sigma_{deadTime} = \frac{\sqrt{\sum_{i=1}^{16} \sigma_x(\tau_m(i))^2}}{T} = \sigma_{deadTime} = 0.4504 \cdot 10^{-16}$$

End Date of each measurement (MJD)	Dead Time Duration second $\tau_m(i)$	$\sigma_x(\tau_m(i))$
53489,642361111	592,00001	9.1258e-13
53490,939583333	41548,00001	4.0802e-11
53492,758333333	46418	4.4781e-11
53493,759027778	2040,00001	2.6290e-12
53494,615277777	20,00003	7.0953e-13
53495,457638889	407,00002	6.6501e-13
53496,622222222	50,00003	7.0953e-13
53497,764583333	392,99999	6.6501e-13
53498,738888889	480,00002	7.7530e-13
53499,740972222	52,99999	7.0953e-13
53500,700000000	619,00002	9.1258e-13
53501,715972222	474,00003	7.7530e-13
53502,652083333	29,00002	7.0953e-13
53503,552777777	684,00003	1.0533e-12
53504,447916667	20266,00001	2.2865e-11
53505,682638889	10508,00001	1.2946e-11

Table 4: Statement of the dead times of $H_{\text{Maser}} 40 0805 - \text{FO2}$ measurements between MJD 53339 and MJD 53399

With taking $\sigma_{link_Maser} = \sqrt{\sigma_{link_lab}^2 + \sigma_{deadTime}^2}$ one obtains $\sigma_{link_Maser} = 0.1097 \cdot 10^{-15}$

Linear Regression on the frequency measurements on period MJD 53489-53504

One calculates the linear regression by the algorithm of weighted least squares by statistical uncertainty of each frequency differences measurements:

$$y_k = a_1 + a_2 t$$

Figure 9 gives the representation of frequency measurements and the linear fit resulting from weighted least squares by inverse of squares statistical uncertainty $1/\sigma_{Ai}^2$.

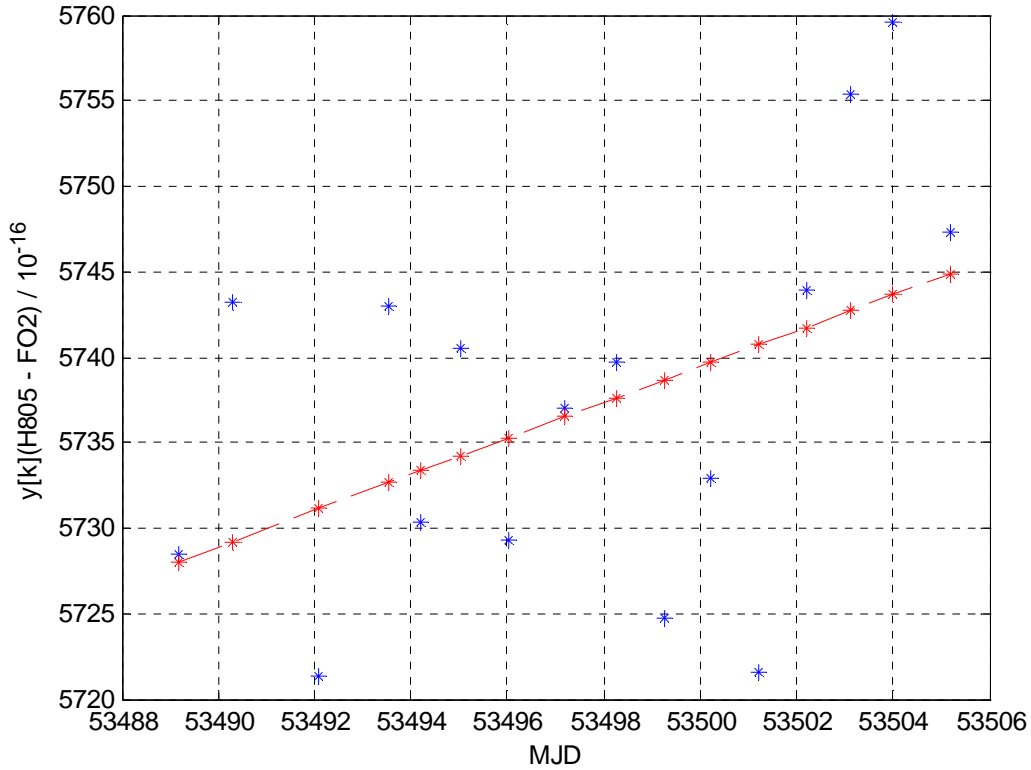


Figure 9: linear regression on the frequency $y(HMaser-FO2)$ between MJD 53489 and 53504 weighted by uncertainty : $1/\sigma_{Ai}^2$

Summary of statistical terms:

Coefficient a1 = -5,0616994214963e-012
 Coefficient a2 = 1,05339148566748e-016
 sigma(a1) yk (FO2) = 5,63993525804634e-013
 sigma(a2) yk (FO2) = 1,0542377756269e-017

Covariance Matrix:

3,18088697149542e-025 -5,94583277792173e-030
 -5,94583277792173e-030 1,11141728755876e-034

Mean date of measurements = 53497,173885
Frequency mean by linear fit y_FO2 = 5,73647326276877e-013
 Uncertainty propagation at t_moyen uc_y_FO2 = 5,01964264933441e-017

Degree of Freedom DEF = 14
 Mean Square Error = Chi2/DEF = 29,2360158001926
 Birge ratio Rb (chi2/DEF)^1/2 = 5,40703391890532
 Limit of Birge ratio Rb = 1+sqrt(2/DEF) = 1,37796447300923
 Probability of a sample y(Maser-FO2) being superior of Chi2|DEF = 6,736782582260394e-079
 SSR Sum Square of Residues = 1,52114938492801e-029
 RMS Root Mean Square of Residues = 3,90019151443619e-015
Allan Deviation extrapolated at T with assumption of White Frequency Noise = 2,433119825108e-016
 T (seconds) = total duration = 1468330,99997712
 Phase difference on the period of integration = 8,42324910943111e-007
 tau0 (mean time between measurements) = 91771 (seconds)

High order Polynomial fit on the frequency measurements on period MJD 53489-53505

One calculates the polynomial fit order $M \geq 2$ by the algorithm of least squares on each frequency differences measurements:

$$y = \sum_{i=0}^M p_{i+1} t^{(M-i)}$$

For 16 data measurements represented on figure 10, with interval duration of 1468331 seconds during MJD 53489,0-53505,0 period. With a polynomial of order $M=5$ we have smoothed the maser noise on 5×91771 s or about 5 days. We obtain the polynomial fit represented on figure 11.

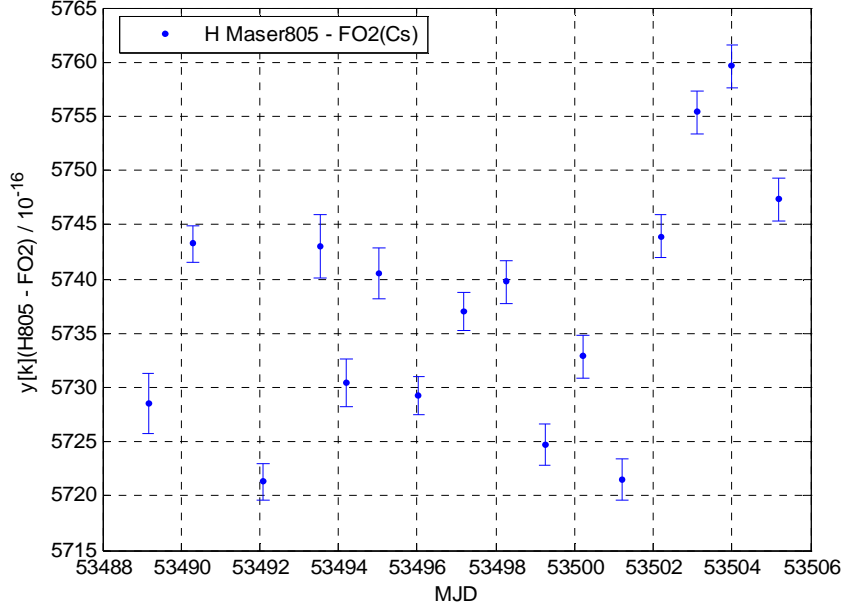


Figure 10: frequency differences & statistical uncertainties of $y(H805-FO2)$, $\tau_0 = 91771s$, MJD 53489 - 53505

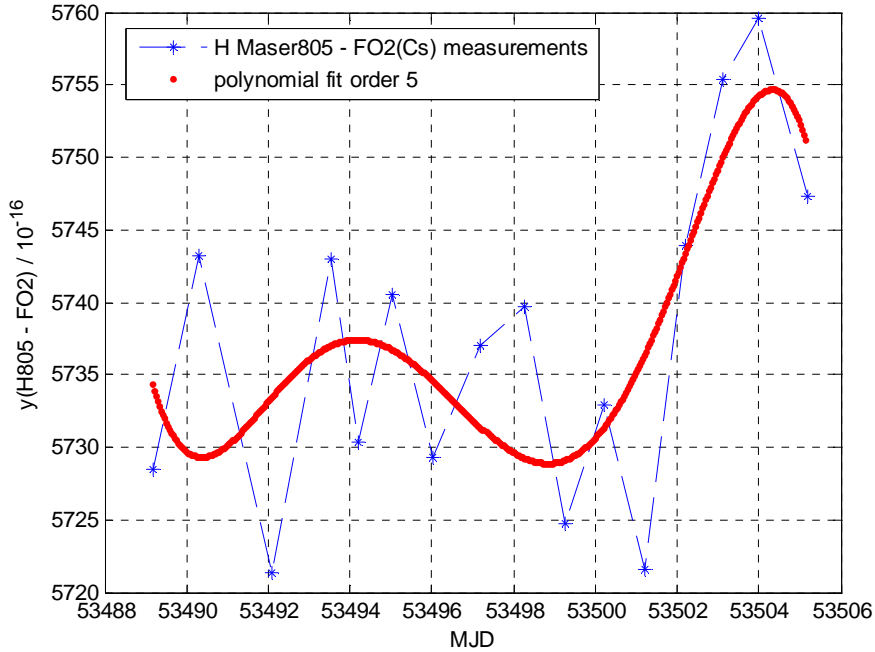


Figure 11: frequency differences $y(H816-FO2)$ and the order 5 polynomial fit MJD 53489 - 53505

By integrating the fit polynomial from 53489 to 53505 we obtain an averaging frequency $\boxed{v_{\text{mov}}(H805-FO2) = 5737,02 \times 10^{-16}}$.

Statistical uncertainty is evaluated by the frequency stability analysis of FO2 fountain. Figure 12 shows an overlapping Allan deviation for the residuals of linear fit and of polynomial fit and laws of white noise frequency modulation of $2,8 \times 10^{-13} \tau^{-1/2}$ modelling of Maser noise and of $2,8 \times 10^{-14} \tau^{-1/2}$ modelling of fountain noise limit. An extrapolated value at the total duration 16,99457 days is obtained by law $\sigma_y(\tau \approx 17 \text{ d})_{\text{Maser}} = 2,31 \times 10^{-16}$ representing the instability of Maser and law $\sigma_y(\tau \approx 17 \text{ d})_{\text{FO2}} = 2,31 \times 10^{-17}$ representing FO2 noise with cryogenic oscillator.

By taking the fountain noise instability value extrapolated and added with the statistical uncertainty σ_A obtained from each measurement

$$\sigma_A = \sqrt{\frac{1}{\sum_{i=1}^n \frac{1}{\sigma_{Stat_i}^2 + \sigma_{Collision_i}^2}}}$$

resulting in $\sigma_A = 0,498 \times 10^{-16}$ we finally obtain the statistical uncertainty of mean frequency $y_{\text{moy(H816-FO2)}} = 5737,02 \times 10^{-16}$ is:

$$u_A = \sqrt{\sigma_A^2 + \sigma_y(\tau = 17 \text{ d})_{\text{FO2}}^2}$$

$$u_A = 0.549 \times 10^{-16}$$

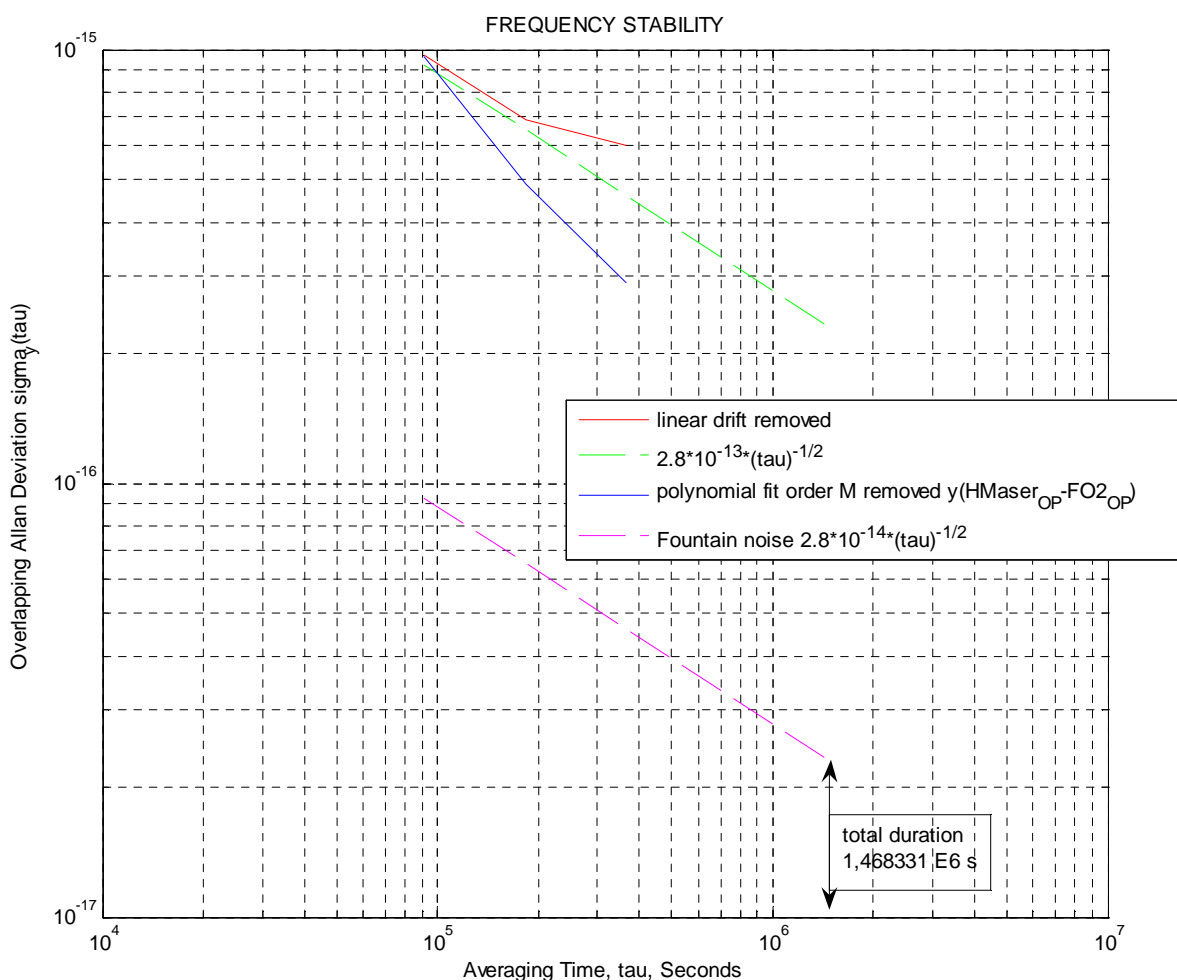


Figure 12: Comparison of frequency stability $y(\text{HMaser805} - \text{FO2})$ polynomial order 1 and order $M=5$ removed from MJD 53489 to MJD 53505

Mean Frequency computed by phase differences

Figure 13 shows the evolution of the differences in fractional frequency $y(t)$. At each period of integration is evaluated a frequency \bar{y}_k corresponding to the interval $t_{k+1} - t_k$. The relation binding the variations of phase and the instantaneous frequency deviations is given by

$$y_k = \frac{x_{k+1} - x_k}{t_{k+1} - t_k} \quad (1)$$

$$y(t) = \frac{V_{HMaser} - V_{FO2}}{V_0}$$

$$v_0 = 9,192631770 \text{ GHz}$$

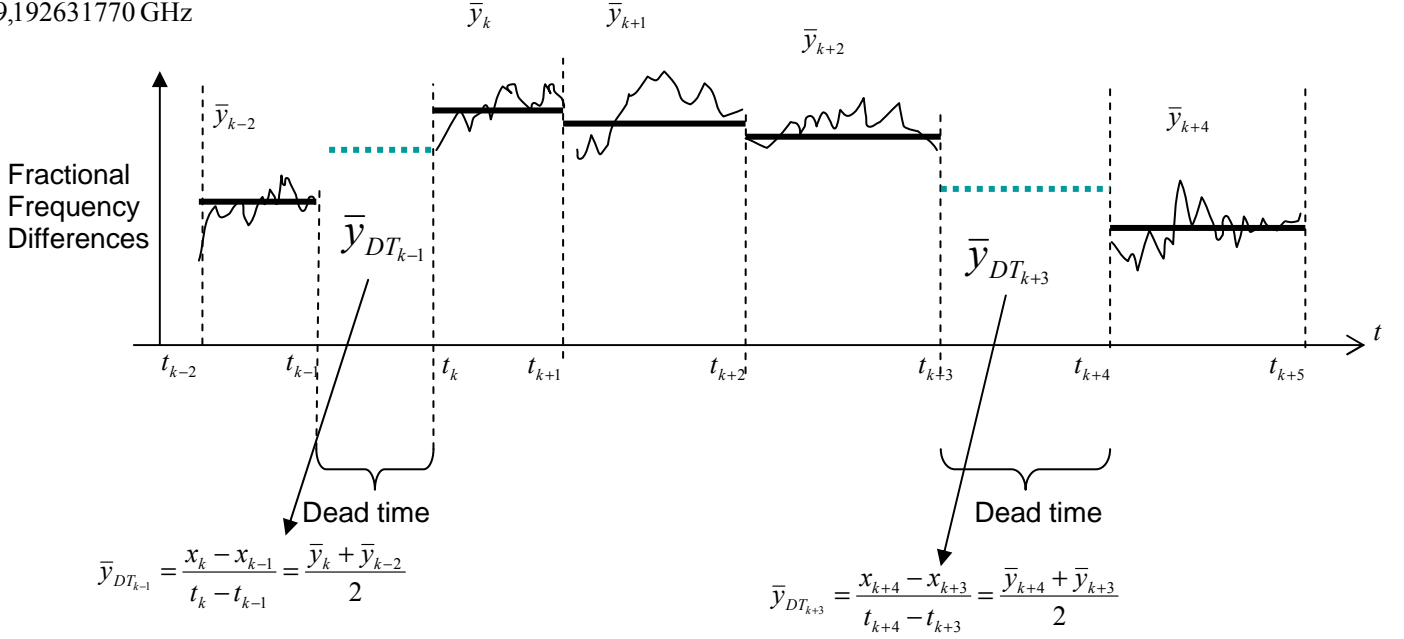


Figure 13: contribution of frequency measurements on the mean frequency calculated

By using equation (1) we have $x_{k+1} - x_k = (t_{k+1} - t_k) y_k$

and for addition of consecutive phase differences we find $\sum_{k=1}^N (x_{k+1} - x_k) = x_{N+1} - x_1 = \sum_{k=1}^N (t_{k+1} - t_k) y_k$

During the dead time we have evaluated the mean frequency by interpolating the mean frequency between two neighbouring intervals of integrations noted:

$$y_{DT_{m-1}} = \frac{1}{2} y_m + \frac{1}{2} y_{m-1} \quad (2)$$

The contributions of N duty intervals with the frequency measurements y_k and M idle intervals with the mean frequency extrapolating between two neighbouring intervals of integration y_{DT} give the summation

$$\left(\sum_{k=1}^N (t_{k+1} - t_k) y_k \right) + \left(\sum_{m=1}^M (t_{m+1} - t_m) y_{DT_m} \right) = x_{fin} - x_{deb} \quad (3)$$

$$y_{moy} = \frac{x_{fin} - x_{deb}}{86400 \text{ MJD}_{fin} - 86400 \text{ MJD}_{deb}} \quad (4)$$

Where $(x_{fin} - x_{deb})$ represents the phase variation between the whole period of integration.

The evaluation of statistical uncertainty on each phase differences data extracted from fractional frequency differences, as we have in presence of white frequency noise (WFM) in each period of measurement, is given by the expression

$$\sigma_x(\tau_i)^2 = \sigma_y(\tau_i)^2 \tau_i^2$$

For the whole period T of measurement that gives in frequency instability

$$\sigma_y(\tau) = \frac{\sqrt{\sum_{i=1}^N \sigma_y(\tau_i)^2 \tau_i^2}}{T}$$

With N=16, from the 29th April to 15th May 2005 and $T = 86400 \text{ MJD}_{fin} - 86400 \text{ MJD}_{deb} = 1468331$ seconds it gives

$$\sigma_y(\tau) = \frac{\sqrt{\sum_{i=1}^{16} \sigma_y(\tau_i)^2 \tau_i^2}}{T} = 0.466 \cdot 10^{-16}$$

$$\sigma_A = 0.466 \cdot 10^{-16}$$

The evaluation of the mean frequency between two intervals of integrations during the period from MJD 53489 to MJD 53505 is given by equation (2) and calculated for frequency fluctuation difference measurements. Figure 14 shows the frequency differences between H_Maser 40 0805 and FO2 (blue plus) and the mean frequency during dead times (magenta stars).

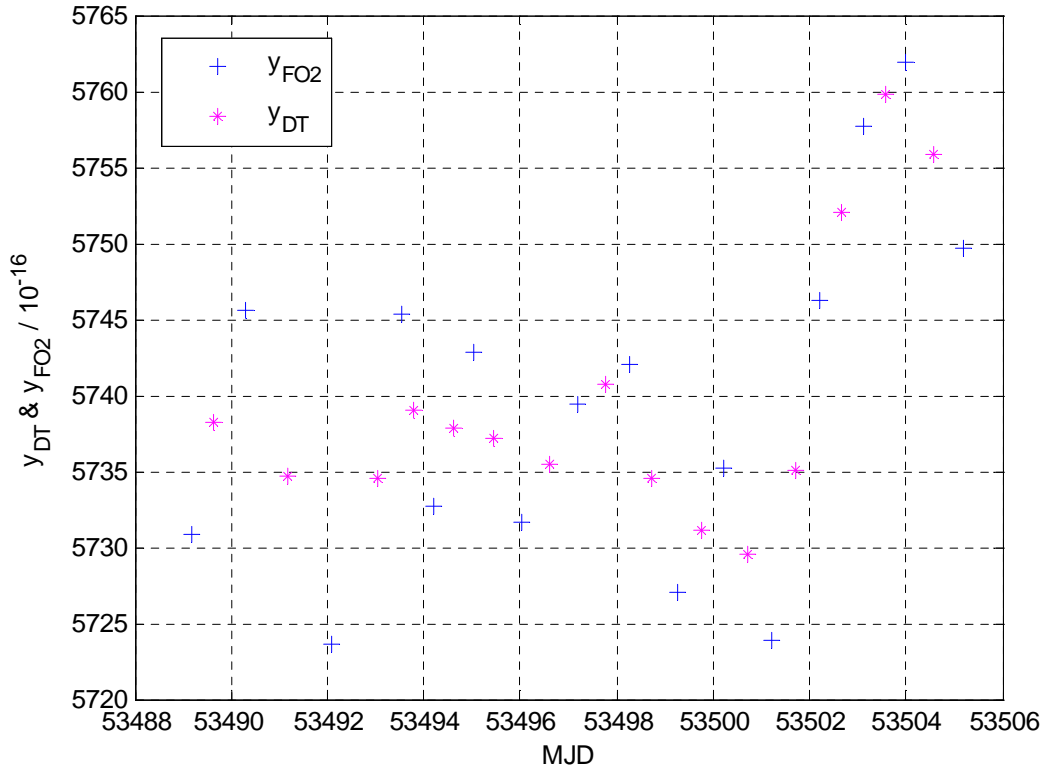


Figure 14: frequency differences H_Maser40 0805 and FO2 from MJD 53489 up to MJD 53505

From equation (3) we find the phase difference over the whole period of integration

$$x_{fin} - x_{deb} = 0.842668 \text{ } \mu\text{s}$$

This value is replaced in equation (4) above for computation of y_{moy} during this period. We find

$$y_{moy} = 0.573661 \cdot 10^{-12}$$

Mean Frequency between H Masers 40 0805 and 40 0816 computed by phase differences over MJD 53405 to 53509

On figure 15 is shown the evolution of the differences between phase differences $x_{[k]}(\text{H805}) - x_{[k]}(\text{H816})$ with a periodic measurement of 100s. From $\text{MJD}_{\text{deb}} 53405,60327$ up to $\text{MJD}_{\text{fin}} 53508,99886$ results $N=89331$ samples of 105 days.

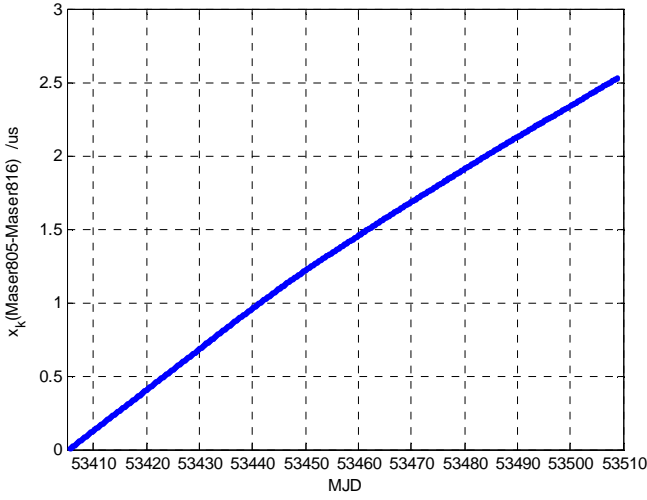


Figure 15: Phase differences Maser805-Maser816, MJD 53405 up to MJD 53509

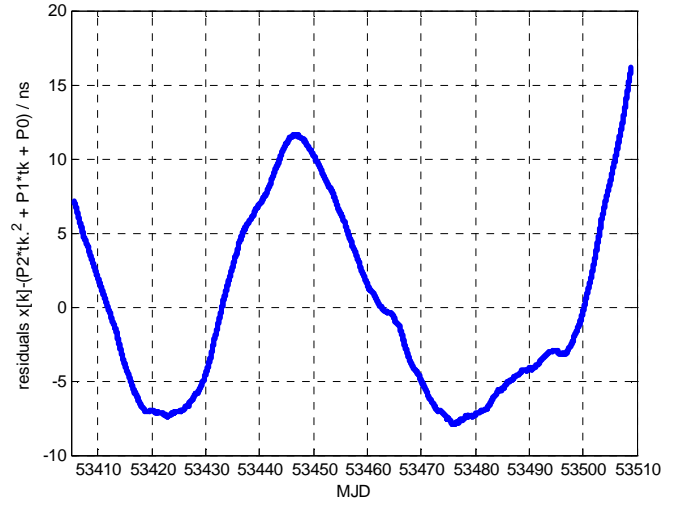


Figure 16: residuals of phase between Masers after quad fit removed, MJD 53405 up to MJD 53509

By using a second order polynomial fitting the phase differences data $x_{[k]}(\text{H805}) - x_{[k]}(\text{H816})$: $x(t) := P_1 t^2 + P_2 t + P_3$

$$P1 = -4.95172307516524e-011 \quad P2 = 5.31848119810025e-006 \quad P3 = -0.14280571322493$$

The mean frequency with this polynomial fit order 2 over the phase differences is given by:

$$y_{\text{moy}} = \frac{1}{86400} \left(\frac{1}{\text{MJD}_{\text{fin}} - \text{MJD}_{\text{deb}}} \int_{\text{MJD}_{\text{deb}}}^{\text{MJD}_{\text{fin}}} 2 P_1 t + P_2 dt \right) \text{ which is equivalent to}$$

$$y_{\text{moy}} = \left(\frac{1}{86400} \text{MJD}_{\text{deb}} + \frac{1}{86400} \text{MJD}_{\text{fin}} \right) P_1 + \frac{1}{86400} P_2$$

Figure 16 shows residuals obtained after this quadratic fit removed. The 24 ns pick to pick residuals results to a frequency instability over the 53405 to 53509 period of 105 days of $2,70 \times 10^{-15}$

$$\rightarrow (y_k)_{\text{moy}} = 2820,16 \times 10^{-16} \pm 27,0 \times 10^{-16}$$

By taking a restrictive period of 16 days 53489,0 to 53505,0 with 2ns pick to pick residuals we find frequency instability of $1,446 \times 10^{-15}$

$$\rightarrow (y_k)_{\text{moy}} = 2446,86 \times 10^{-16} \pm 15,38 \times 10^{-16}$$

Frequency difference between Masers obtained by first phase difference between beginning and ending of the whole period gives $\rightarrow (y_k)_{\text{moy}} = 2830,20 \times 10^{-16}$ with statistical uncertainty corresponding to $u_A(y_k)_{\text{moy}} = 2\sigma_{\text{meas}}/T$ with $\sigma_{\text{meas}} = 2\text{ps}$ of the time interval counter Stanford Research SR620 and $T = 8933379\text{s}$ $\rightarrow u(y_k)_{\text{moy}} = 0,45 \times 10^{-18}$.

$$y_{H805 - H816} = 0.283020 \times 10^{-12}$$

$$u_A(y_{H805 - H816}) = 0.45 \times 10^{-18}$$

By taking the restrictive period of 16 days 53489.0 to 53505.0 we find

$$y_{H805 - H816} = 0.245593 \times 10^{-12}$$

$$u_A(y_{H805 - H816}) = 0.289 \times 10^{-17}$$

Systematic error is evaluated with the time interval error of the time interval counter Stanford Research SR620:

$$\text{Error} < \pm (500 \text{ ps typ. [1 ns max.] + Timebase Error ' Interval + Trigger Error)$$

Considering the 3σ time interval error equal to 1 ns, the $1\sigma = 333,33\text{ps}$. The evaluation of Time base Error is 1,35ps and the Trigger error is 0,23ps on input A and 0,23ps on input B of the counter. So we obtain $\sigma_{x(\text{Counter})}(1\sigma) = 335 \text{ ps}$ that is divided by a factor 100 corresponding to the phase difference multiplication used with the counter.

From the frequency mean resulting from the first phase difference between the whole interval periods, the uncertainty is computed by

$$\sigma_B(y_k)_{\text{moy}} = 2\sigma_{x(\text{Counter})}/T \rightarrow u_B(y_{H805-H816}) = 0.75281 \cdot 10^{-18}$$

By taking the restrictive period of 16 days 53489,0 to 53505,0 we find

$$\sigma_B(y_k)_{\text{moy}} = 2\sigma_{x(\text{Counter})}/T \rightarrow u_B(y_{H805-H816}) = 0.47857 \cdot 10^{-17}$$

Frequency difference between the H Maser 40 0805 & H Maser 40 0816 from MJD 53489 to 53505 is resumed below:

$$y_{H805-H816} = 0.245593 \cdot 10^{-12} \quad u_A(y_{H805-H816}) = 0.289 \cdot 10^{-17} \quad u_B(y_{H805-H816}) = 0.47857 \cdot 10^{-17}$$

This result can be verified in consistency with the daily measurements of phase differences between Masers and the atomic local time scale UTC(OP). The differences between the phase differences $x_k(\text{H805-UTC(OP)})$ and $x_k(\text{H816-UTC(OP)})$ is plotted on figure 17 from MJD 53405 and MJD 53509, 1 sample by day, 105 days.

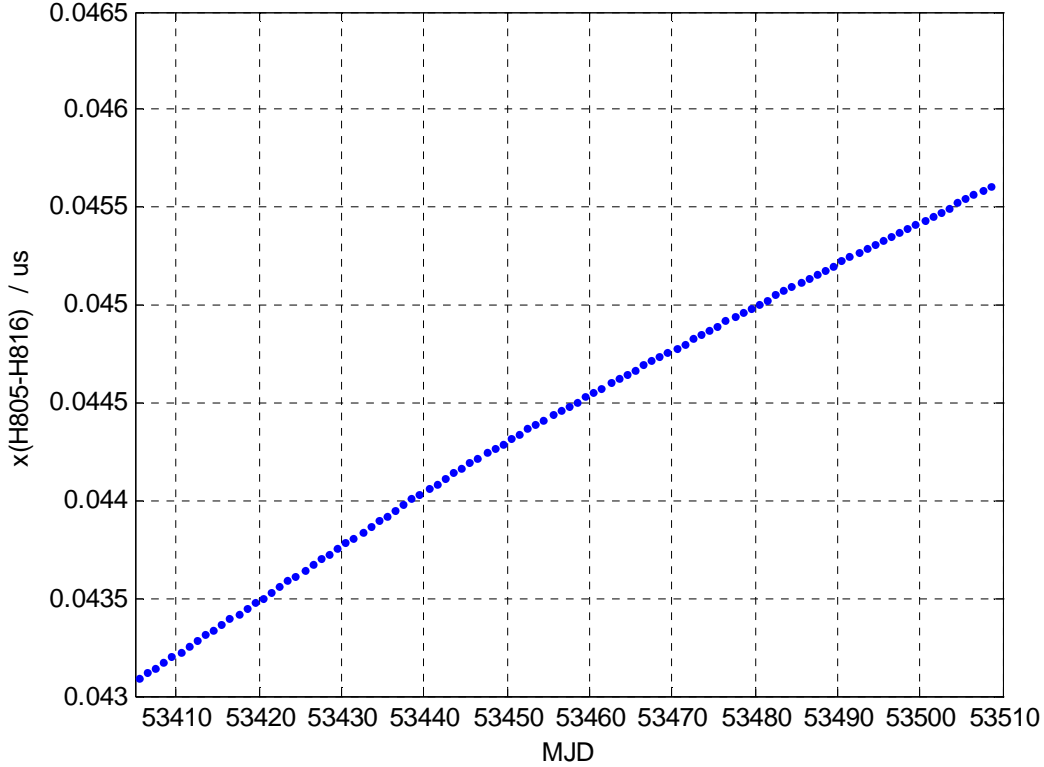


Figure 17: Phase differences (Maser805-UTC(OP)) - (Maser816 - UTC(OP)), MJD 53405 up to MJD 53509

Frequency difference between Masers obtained by phase difference between beginning and ending of the 53405- 53509 period gives $\rightarrow (y_k)_{\text{moy}} = 2831,71 \times 10^{-16}$ with statistical uncertainty corresponding to $u_x = \sqrt{2} \cdot u_x(t)$ with $u_x(t) = 150\text{ps} \rightarrow u_x = 212\text{ps}$ and over the 105 days of the whole period $u_y(y_{\text{moy}}) = 0,23 \times 10^{-17}$. The mean frequency obtained by these daily phase difference measurements Maser-UTC(OP) is resumed by:

$$\rightarrow (y_k)_{\text{moy}} = 2831,71 \times 10^{-16} \pm 0,023 \times 10^{-16}$$

The frequency difference between these two frequency averages is $-1,51 \times 10^{-16}$ that is compatible with their respective uncertainties.

By taking the restrictive period of 16 days 53489 to 53505 we find

$$\rightarrow (y_k)_{\text{moy}} = 2461,41 \times 10^{-16} \pm 1,53 \times 10^{-16}$$

The frequency difference between these two frequency averages is $-5,48 \times 10^{-16}$ that is compatible with their respective uncertainties.

REFERENCES

[ref. 1] - C. Vian, P. Rosenbusch, H. Marion, S. Bize, L. Cacciapuoti, S. Zhang, M. Abgrall, D. Chambon, I. Maksimovic, P. Laurent, G. Santarelli, A. Clairon of Obs. Paris, SYRTE, A. Luiten, M. Tobar, Univ. W. of Australia School of Physics, C. Salomon of LKB, "BNM-SYRTE Fountains: Recent Results", **CPEM 2004, Proceedings IEEE Transactions on Instrumentation & Measurement, Vol. 54, NO. 2, April 2005.**

[ref. 2] - F. Pereira Do Santos, H. Marion, M. Abgrall, S. Zhang, Y. Sortais, S. Bize, I. Maksimovic, D. Calonico, J. Grünert, C. Mandache, C. Vian, P. Rosenbusch, P. Lemonde, G. Santarelli, Ph. Laurent and A. Clairon of BNM-SYRTE, C. Salomon of LKB, "Rb and Cs Laser Cooled Clocks: Testing the Stability of Fundamental Constants". **Proceedings IEEE 2003, EFTF Tampa May 2003, p 55-67.**

[ref. 3] - P. Wolf of BNM SYRTE, C.J. Bordé of LPL, "Recoil effects in microwave Ramsey spectroscopy", arxiv: **quant-ph/0403194.**

[ref. 4] - F. Pereira Do Santos, H. Marion, S. Bize, Y. Sortais, A. Clairon, and C. Solomon "Controlling the Cold Collision Shift in High Precision Atomic Interferometry" of, **Phys, Rev, Lett, 89,233004 (2002).**

[ref. 5] - J. Vanier, C. Audouin, « The Quantum Physics of Atomic Frequency Standards », **Adam Hilger, Bristol & Philadelphia (1989).**

[ref. 6] - R. Schröder, U. Hübner and D. Griebisch, "Design and Realization of the Microwave Cavity in PTB Caesium Atomic Clock CSF1" **IEEE Trans. Instrum. Meas., vol. 49, p.383, 2002.**

[ref. 7] - L. Cutler *et al*, "Frequency pulling by hyperfine σ - transitions in cesium atomic frequency standards, **J. Appl. Phys. Vol. 69, pp. 2780, 1991.**

[ref. 8] - A. Bauch, R. Schröder "Frequency shift in Caesium Atomic Clock due to Majorana transitions", **Annalen der Physik, vol. 2, pp. 421, 1993.**

[ref. 9] – H. Marion thèse de doctorat de l'Université de Paris 6 (Mars 2005)